Photon-Assisted Tunneling in a Carbon Nanotube Quantum Dot

C. Meyer, Ch. Spudat, C. M. Schneider

IFF-9: Electronic Properties
CNI: Center of Nanoelectronic Systems for Information Technology

Electronic devices become smaller and smaller. Silicon based technology as we know it today will reach its limit within the next decade. To go beyond this limit, we investigate new materials and methods for information processing. In this context, we are interested in the transport properties of carbon nanotubes, which are ideal one dimensional ballistic conductors. Electron spins in carbon nanotubes (CNTs) are expected to have long relaxation times due to the small spin-orbit coupling and the possible absence of nuclear spins. This could make CNT quantum dots very suitable candidates for a solid state quantum computing system [1]. We study photon-assisted tunneling (PAT) in a CNT quantum dot under microwave irradiation (20 to 60 GHz) as a first step towards high-frequency control over such a spin qubit.
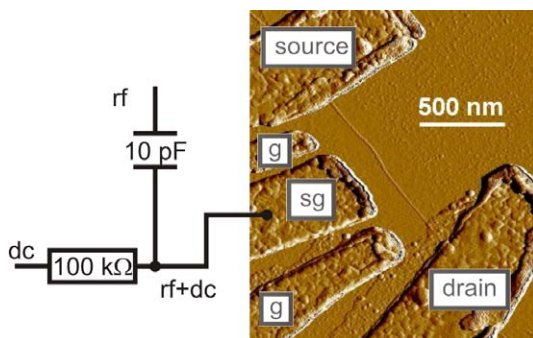

FIG. 1: Schematic layout of the device with low temperature bias-tee and AFM picture of a similar device as the one used for the experiments discussed here. The actual device has a total nanotube length of 940 nm between the Al contacts. The side gate (sg), which is flanked by two guard electrodes (g), has a width of 410 nm, and its distance to the CNT is about 200 nm.

Single-walled carbon nanotubes (SWCNTs) are grown using chemical vapor deposition (CVD) on a patterned Si/SiO$_2$ substrate. The quantum dot is formed between Aluminum source/drain contacts, and the potential can be tuned using an Aluminum side-gate (see Fig.1). The low work function of Aluminum ensures high tunnel barriers at low temperatures. We achieved tunneling rates $\Gamma << h\nu$, with ν the frequency of the rf signal, which allows us to clearly resolve the microwave-induced side peaks [2]. All measurements are performed at the base temperature of a dilution refrigerator. The high-frequency signal and dc gate voltage are added with a bias-tee at base temperature ($\sim$25 mK), and applied to the side gate. Two guard electrodes surrounding it are set to ground and suppress the capacitive coupling of the side gate to source and drain contacts. Fig.2 shows measurements of current versus gate voltage of the unperturbed Coulomb peak (dashed curve) and the peak splitting under high-frequency irradiation. As expected, the total splitting between the extra resonances in the current is $2h\nu$ and increases linearly with frequency. The insets of Fig.2 describe the PAT processes of a single-level system for the left and right side peak, respectively. Left of the main Coulomb resonance, when the quantum dot is in its N electron state and the electrochemical potential of the $N \leftrightarrow N + 1$ resonance is above the bias window, an electron in the left lead can absorb a photon and tunnel onto the dot. This electron can then leave the dot to both sides with the same probability, but it contributes to the current only if it tunnels to the right lead. This process is frequency dependent, because as soon as an electron from the right lead can also absorb a photon and tunnel onto the dot, the net current from these two processes will be zero. To the right of the main resonance, the quantum dot is in its $N + 1$ stable state and an electron on the dot can absorb a photon and tunnel out to the right lead. An electron can then enter from the Fermi sea of either of the leads and refill the level, but it contributes to the current only when entering from the left.

We then perform excited-state spectroscopy with PAT in order to study the frequency independent peaks at different microwave power and ν = 40.8 GHz. These peaks, at positions ϵ_{bc} = -83(7) μeV and ϵ_{ad}= 70(7) μeV relative to the Coulomb peak ϵ_{ac}, have their origin in tunneling through excited states initiated by a PAT process and are more apparent at high power while the main resonance decreases. Similar behavior has been observed in GaAs dots. We emphasize, however, that the PAT-induced excited state peak denoted here as bc has not been reported before, to the best of our knowledge. At the ϵ_{ad} peak tunneling occurs between the N electron ground state and an N+1 excited state, in case of the ϵ_{bc} peak, tunneling occurs between an N-electron excited state and the N+1 ground state.
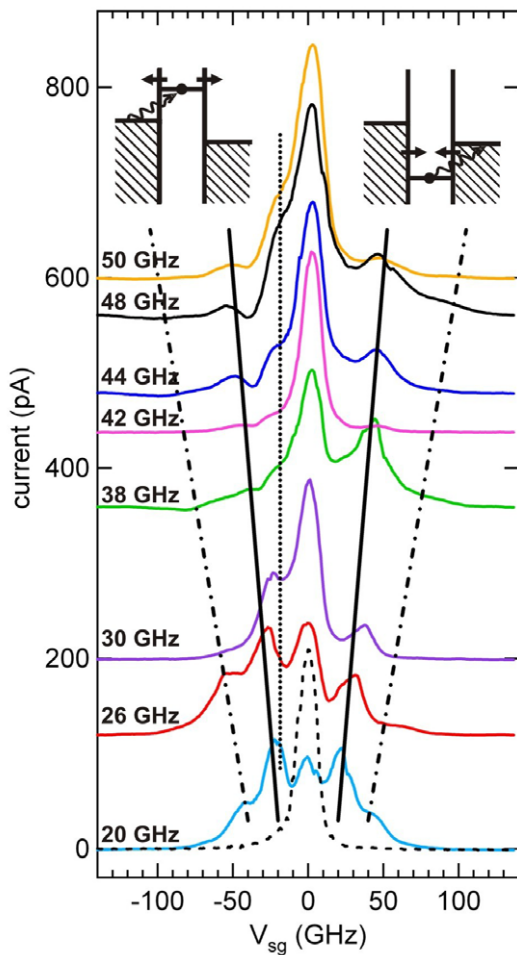
FIG. 2: Photon-assisted tunneling at different frequencies; ac source voltage amplitude V_{ac} = 71 mV (-10 dBm), bias voltage V_{SD} = 50 μeV. The dc side gate voltage V_{SG} is swept from 266.4 mV to 300 mV, and converted to an energy scale in GHz, using a conversion factor for the gate voltage to energy of $C_g/C_\Sigma \sim 0.03$. The Coulomb peak measured without rf irradiation (dashed curve) is compared to the traces with rf irradiation. The insets describe the basic PAT process below (left inset) and above (right inset) the main resonance. The black straight lines are guides to the eye for the one-photon satellites (solid) at positions $\pm h\nu$ away from the main Coulomb resonance, the two-photon side peaks (dash-dotted), and a frequency independent excited state that is visible at higher frequencies (dotted).

quantum dots as well and was explained by intra-dot excitations [4].

These observations are the first steps towards high-frequency control of carbon nanotube quantum dots, which is vital for using spin in nanotubes for quantum information processing.
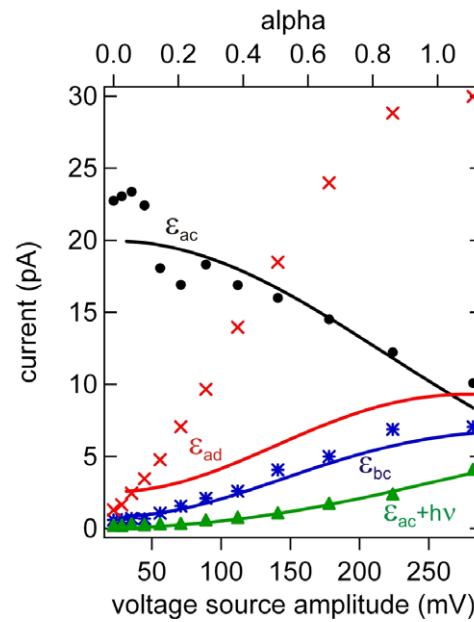

FIG. 3: Comparison between measured current (markers) and simulated current (solid line) for different peaks for differents microwave power at ν = 40.8 GHz.

[1] D. Loss, D. DiVincenzo, Phys. Rev. A **57**, 120 (1998)

[2] L. P. Kouwenhoven, S. Jauhar, K. McCormick, D. Dixon, P. L. McEuen, Yu. V. Nazarov, N. C. van der Vaart, C. T. Foxon, Phys. Rev. B **50**, 2019 (1994)

[3] C. Meyer, J. M. Elzermann, L. P. Kouwenhoven, Nano Letters **7**, 295 (2007)

[4] Ph. Brune, C. Bruder, H. Schoeller, Phys. Rev. B **56**, 4730 (1997)

For better understanding of the power dependence of the excited states, we compare our data to the simulation of a model system described in [3]. In Fig.3, we compare the result of the simulation (solid lines) with the data (markers). We find good agreement for the main resonance (black), the ϵ_{bc} peak (blue), and the peak of $\epsilon_{ac} + h\nu$ (green) assuming a small asymmetry in the coupling of the microwaves $\alpha = \frac{eV}{h\nu}$ to the barriers ($\alpha_l = 0.95\alpha_r$). The functional dependence of the peak ϵ_{ad} (red) on the microwave power is the same in the simulation as in the data. However, the current is strongly enhanced compared to the simulation. A similar behavior has been observed for GaAs